Journal of Experimental and Theoretical Physics, Vol. 93, No. 5, 2001, pp. 977–984.
Translated from Zhurnal Éksperimental'noĭ i Teoreticheskoĭ Fiziki, Vol. 120, No. 5, 2001, pp. 1126–1134.

ATOMS, SPECTRA, RADIATION

Localized Electromagnetic Modes and the Transmission Spectrum of a One-Dimensional Photonic Crystal with Lattice Defects

S. Ya. Vetrov[a, *] and A. V. Shabanov[b]

[a]*Krasnoyarsk State Technical University, Krasnoyarsk, 660074 Russia*
[b]*Kirenskii Institute of Physics, Siberian Division, Russian Academy of Sciences, Akademgorodok, Krasnoyarsk, 660036 Russia*
**e-mail: chery@escape.akadem.ru*

Received December 21, 2000

Abstract—The properties of localized electromagnetic modes in a one-dimensional photonic crystal with a structural defect layer were studied. The role of the defect was played by an anisotropic nematic liquid crystal layer. The frequency and the damping factor of defect modes were shown to substantially depend on the defect layer thickness and the orientation of the optical axis of the nematic. The transmission spectra of photonic crystals with one and two lattice defects were studied. Taking into account the special feature of nematic liquid crystals distinguishing them from usual crystals, namely, large permittivity anisotropy, it was shown that the transmission spectrum of the photonic crystal could be controlled by varying the orientation of the optical axis of the nematic, for instance, under the action of an external electric field. *© 2001 MAIK "Nauka/Interperiodica".*

1. INTRODUCTION

In recent years, much attention has been given to photonic crystals [1], which are a special class of artificial structures with periodic dielectric property variations on a spatial scale of the order of the optical wave length. Depending on the periodicity dimension, photonic crystals are classified as one-, two-, and three-dimensional. The value of the concept of photonic structures lies in the possibility of studying physical phenomena from a new standpoint based on the traditional ideas of the physics of solids and electromagnetism. There is a close formal analogy between the theory of electromagnetic radiation propagation in periodic media and the quantum theory of electrons in crystals. The band structure of the energy spectrum of electrons in crystals caused by Bragg reflection of electrons is similar to the structure of the spectrum of a photonic crystal. Many interesting and potentially useful phenomena are related to the presence of photonic band gaps in photonic crystals and their unusual dispersion properties. Photonic crystalline structures make it possible to solve some fundamental problems, for instance, problems related to controlling spontaneous light emission from atoms and molecules [2–4] and localizing and channeling light [1, 5–11]. In practical applications, photonic band gap structures are extensively used in creating photonic crystal waveguides [8, 12, 13], superfast optical switches [14, 15], Bragg reflectors [16], detectors [17], and optical schemes [18, 19]. Note that the ability to use electrooptic effects for controlling photonic band gap structures is of importance for many practical applications. It was shown in [20] for three-dimensional photonic band gap structures formed with nematic liquid crystal inclusions that the transmission spectrum of a photonic crystal could be effectively controlled by varying the orientation of the optical axis of the nematic. Earlier [21], surface electromagnetic waves at the interface between an isotropic medium and a superlattice of alternating isotropic and nematic liquid crystal layers were studied. It was shown that the characteristics of surface waves could be effectively controlled. Volume electromagnetic waves in infinite and bounded superlattices comprising alternating isotropic and nematic layers were studied in [22]. It was shown that the spectrum of electromagnetic waves in superlattices could be considerably modified by changing the orientation of the optical axis of nematic liquid crystals. The possibility of effectively controlling the electromagnetic wave transmission coefficient by changing the orientation of the director of nematic liquid crystals was also noted.

In this work, we study the properties of localized electromagnetic modes in a one-dimensional photonic crystal with a defect structural layer. The role of the defect layer is played by an anisotropic nematic liquid crystal layer. We also study the transmission spectra of photonic crystals with one and two lattice defects. We show that the characteristics of localized modes and the transmission spectrum of a photonic crystal can be controlled by changing the orientation of the optical axis of the nematic.

Sections 2 and 3 contain a description of the theory used to perform the numerical simulation whose results are given in Section 4.

1063-7761/01/9305-0977$21.00

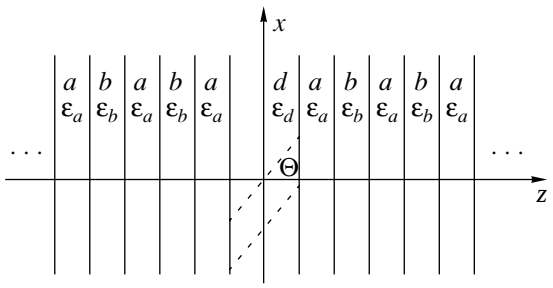

Fig. 1. One-dimensional photonic band gap structure with a lattice defect.

2. EQUATIONS FOR LOCALIZED MODE FREQUENCIES AND FORMS

The photonic band gap structure that we consider is an infinite layered medium comprising alternating isotropic layers of two materials with a structural defect (Fig. 1). The role of the defect layer is played by a nematic liquid crystal layer denoted by "*d*." The thickness of this layer is W_d, and θ is the angle between the optical axis of the nematic and the *z* axis. The nematic liquid crystal layer is inserted between two semibounded superlattices whose unit cell consists of materials *a* and *b* with layer thicknesses W_a and W_b, respectively.

The structure under consideration is characterized by permittivities ε_a and ε_b of layers *a* and *b* and the permittivity tensor of the nematic liquid crystal layer

$$\hat{\varepsilon} = \begin{bmatrix} \varepsilon_\perp \cos^2\theta + \varepsilon_\parallel \sin^2\theta & 0 & \frac{1}{2}\sin(2\theta)\Delta\varepsilon \\ 0 & \varepsilon_\perp & 0 \\ \frac{1}{2}\sin(2\theta)\Delta\varepsilon & 0 & \varepsilon_\perp \sin^2\theta + \varepsilon_\parallel \cos^2\theta \end{bmatrix}, \quad (1)$$

where $\varepsilon_\perp = \varepsilon_{x'x'} = \varepsilon_{y'y'}$, $\varepsilon_\parallel = \varepsilon_{z'z'}$ are the components of the permittivity tensor in principal axes and $\Delta\varepsilon = \varepsilon_\parallel - \varepsilon_\perp$. Further, we only take into account the diagonal components of tensor (1). This is justified if $\theta = 0$ or $\theta = \pi/2$. The Maxwell equations for the anisotropic defect photonic crystal layer on the class of *H*-type fields with frequency ω,

$$\{E_x, H_y\} = \{E_x(z), H_y(z)\}e^{-i\omega t} \quad (2)$$

have the form

$$\left(\frac{d^2}{dz^2} + \frac{\varepsilon_{xx}\omega^2}{c^2}\right)E_x(z) = 0,$$
$$H_y(z) = -\frac{ic}{\omega}\frac{dE_x}{dz}, \quad (3)$$

where *c* is the velocity of light in the vacuum. The equations for *E*-type fields are obtained from (3) by the replacements $E_x(z) \longrightarrow E_y(z)$, $H_y(z) \longrightarrow -H_x(z)$, and $\varepsilon_{xx} \longrightarrow \varepsilon_{yy} = \varepsilon_\perp$. The Maxwell equations for isotropic photonic crystal layers are obtained from (3) by the replacement $\varepsilon_{xx} \longrightarrow \varepsilon_a$ or $\varepsilon_{xx} \longrightarrow \varepsilon_b$.

The geometry of the problem set above makes it possible to adapt the method of studying localized acoustic phonon modes in a superlattice with an isotropic defect layer [23] to our purposes. The solution to the Maxwell equations for an electric field localized in a defect *L* mode can be written in the form

$$E_x(z, t) = E_L(z)\exp(-i\omega_L t), \quad (4)$$

where $E_L(z) \equiv E_x(z)$ is the electric field strength for the localized *L* mode and ω_L is the localized mode frequency. For a photonic band gap structure with a lattice defect, the electric field strength in various layers can be written taking into account general solution (3) to the Maxwell equation for a field in a layer in the form

$$E_L(z) = \begin{cases} f(A^r_{Lj}, B^r_{Lj}, k_{Lj}, z - z^r_{mj})\exp[iq_z(m-1)W] \\ -\frac{W_j}{2} \le z - z^r_{mj} \le \frac{W_j}{2}; \\ f(A_{Ld}, B_{Ld}, k_{Ld}, z - z_d) \\ -\frac{W_d}{2} \le z - z_d \le \frac{W_d}{2}; \\ f(A^l_{Lj}, B^l_{Lj}, k_{Lj}, z - z^l_{mj})\exp[iq_z(m-1)W] \\ -\frac{W_j}{2} \le z - z^l_{mj} \le \frac{W_j}{2}. \end{cases} \quad (5)$$

Here, the $f(A, B, k, z)$ function is defined by the equality

$$f(A, B, k, z) = Ae^{ikz} + Be^{-ikz}, \quad (6)$$

z_d is the coordinate of the center of the defect layer; z^l_{mj} and z^r_{mj} are the coordinates of the centers of the *j*th (*j* = *a*, *b*) layer in the *m*th (*m* = 1, 2, 3, …) period of semiinfinite superlattices from the left and from the right, respectively; $k_{L\mu}$ is given by the equality

$$k_{L\mu} = \frac{\omega_L n_\mu}{c}, \quad \mu = a, b, d, \quad (7)$$

where

$$n_\mu = \sqrt{\varepsilon_\mu}, \quad \varepsilon_d = \varepsilon_{xx} = \varepsilon_\perp \cos^2\theta + \varepsilon_\parallel \sin^2\theta,$$

and Bloch wave number q_z should be complex,

$$q_z = \frac{n\pi}{W} + iq, \quad q > 0, \quad n = 1, 2, 3, \ldots. \quad (8)$$

Here, $W = W_a + W_b$ is the period of the ideal layered medium. The continuity condition for E_x and H_y at the interfaces gives equations for determining the ω_L fre-

quency and the q damping factor of localized modes. These equations have the form

$$\cosh(qW) = (-1)^n\left(\cos\alpha\cos\beta - \frac{1}{2}n_{ba}^{+}\sin\alpha\sin\beta\right), \quad (9)$$

$$(-1)^n\sinh(qW)(2\cos\alpha\cos\beta - n_{da}^{+}\sin\alpha\sin\gamma) - \left(\sin\alpha\cos\beta + \frac{1}{2}n_{ba}^{+}\sin\beta\cos\alpha\right) \quad (10)$$

$$\times(2\sin\alpha\cos\gamma + n_{da}^{+}\sin\gamma\cos\alpha) + \frac{1}{2}n_{ba}^{-}n_{da}^{-}\sin\beta\sin\gamma = 0,$$

where

$$\alpha = k_{La}W_a, \quad \beta = k_{Lb}W_b, \quad \gamma = k_{Ld}W_d,$$
$$n_{ba}^{\pm} = \frac{n_b}{n_a} \pm \frac{n_a}{n_b}, \quad n_{da}^{\pm} = \frac{n_d}{n_a} \pm \frac{n_a}{n_d}.$$

The electric field distribution in localized modes of the photonic crystal structure can be written as

$$E_L(z) = \begin{cases} A_{La}^r f(A_{Ld}, B_{Ld}, k_{Ld}, z - z_d), \\ -\dfrac{W_d}{2} \le z - z_d \le \dfrac{W_d}{2}; \\ A_{La}^r f\left(1, \dfrac{\exp(-iq_zW) - \varphi_1}{\varphi_1}, k_{La}, z - z_{ma}^r\right) \\ \times \exp[iq_z(m-1)W], \quad -\dfrac{W_a}{2} \le z - z_{ma}^r \le \dfrac{W_a}{2}; \\ A_{La}^r f(A_{Lb}^r, B_{Lb}^r, k_{Lb}, z - z_{mb}^r)\exp[iq_z(m-1)W], \\ -\dfrac{W_b}{2} \le z - z_{mb}^r \le \dfrac{W_b}{2}; \\ A_{La}^r f(A_{L\nu}^l, B_{L\nu}^l, k_{L\nu}, z - z_{m\nu}^l)\exp[iq_z(m-1)W], \\ \nu = a, b, \end{cases} \quad (11)$$

where

$$\varphi_1 = \cos\alpha\cos\beta - i\sin\alpha\cos\beta - \frac{1}{2}n_{ba}^{-}(\sin\alpha\sin\beta + i\cos\alpha\sin\beta),$$

$$\varphi_2 = -\frac{i}{2}n_{ba}^{-}\sin\beta,$$

A_{La}^r is the normalization constant, and q_z is given by (9) and (10). Here,

$$\begin{pmatrix} A_{Lb}^r \\ B_{Lb}^r \end{pmatrix} = \hat{\Lambda}^{-1}(c_1, k_{Lb}, -W_b)\hat{\Lambda}(c_1, k_{La}, W_a)\hat{C},$$

$$\begin{pmatrix} A_{Ld} \\ B_{Ld} \end{pmatrix} = \hat{\Lambda}^{-1}(c_1, k_{Ld}, W_d)\hat{\Lambda}(c_1, k_{La}, -W_a)\hat{C},$$

$$\begin{pmatrix} A_{La}^l \\ B_{La}^l \end{pmatrix} = \hat{\Lambda}^{-1}(c_1, k_{La}, W_a)\hat{\Lambda}(c_1, k_{Ld}, -W_d)\begin{pmatrix} A_{Ld} \\ B_{Ld} \end{pmatrix}, \quad (12)$$

$$\begin{pmatrix} A_{Lb}^l \\ B_{Lb}^l \end{pmatrix} = \hat{\Lambda}^{-1}(c_1, k_{Lb}, W_b)\hat{\Lambda}(c_1, k_{La}, -W_a)\begin{pmatrix} A_{La}^l \\ B_{La}^l \end{pmatrix},$$

where

$$\hat{\Lambda}(c_1, k, z) = \begin{pmatrix} e^{ikz/2} & e^{-ikz/2} \\ ic_1ke^{ikz/2} & -ic_1ke^{-ikz/2} \end{pmatrix}, \quad (13)$$

$$\hat{C} = \begin{pmatrix} 1 \\ \dfrac{\exp(-iq_zW) - \varphi_1}{\varphi_2} \end{pmatrix}. \quad (14)$$

3. TRANSMISSION SPECTRUM

The transmission spectrum of a bounded photonic crystal with lattice defects will be studied by the transfer matrix method [24]. Let the permittivities of the layers be written as

$$\varepsilon = \begin{cases} \varepsilon(0) = 1, \quad z < z_0 \\ \varepsilon(1) = \varepsilon_b, \quad z_0 < z < z_1 \\ \varepsilon(2) = \varepsilon_a, \quad z_1 < z < z_2 \\ \ldots \\ \varepsilon(l_1) = \varepsilon_d, \quad z_{l_1-1} < z < z_{l_1} \\ \ldots \\ \varepsilon(l_2) = \varepsilon_d, \quad z_{l_2-1} < z < z_{l_2} \\ \ldots \\ \varepsilon(N) = \varepsilon_b, \quad z_{N-1} < z < z_N \\ \varepsilon(s) = 1. \end{cases} \quad (15)$$

For the structure under consideration, the electric field distribution in layers has the form

$$E_x(n, t) = [A(n)\exp(\alpha(n)(z - z_n)) + B(n)\exp(-\alpha(n)(z - z_n))]\exp(-i\omega t), \quad (16)$$

where $A(n)$ and $B(n)$ are the incident and reflected wave amplitudes, respectively, in the nth layer,

$$\alpha(n) = \frac{\sqrt{\varepsilon(n)}\omega}{c}. \quad (17)$$

The magnetic field distribution in layers can be written as

$$H_y(n, t) = [A(n)\exp(i\alpha(n)(z - z_n)) - B(n)\exp(-i\alpha(n)(z - z_n))]\sqrt{\varepsilon(n)}\exp(-i\omega t). \quad (18)$$

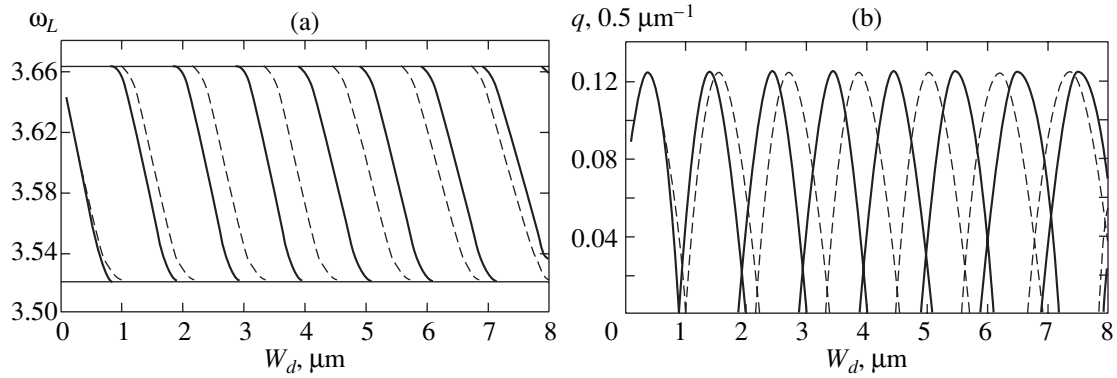

Fig. 2. Dependences of localized mode (a) frequency and (b) damping factor on defect layer thickness. The dashed line corresponds to $n_d = 1.5$ at $\theta = 0$, and the solid line, to $n_d = 1.7$ at $\theta = \pi/2$; ω_L is in c/W units.

The continuity condition for E_x and H_y at the interfaces, $z = z_{n-1}$, gives a system of equations which can be written as the matrix equation

$$\begin{pmatrix} A(n-1) \\ B(n-1) \end{pmatrix} = T_{n-1,n} \begin{pmatrix} A(n) \\ B(n) \end{pmatrix}. \quad (19)$$

Here, the transfer matrix has the form

$$T_{n-1,n} = D^{-1}(n-1)D(n)P(n), \quad (20)$$

where

$$D(n) = \begin{pmatrix} 1 & 1 \\ \sqrt{\varepsilon(n)} & -\sqrt{\varepsilon(n)} \end{pmatrix}, \quad (21)$$

$$P(n) = \begin{pmatrix} e^{-i\alpha(n)\gamma_n} & 0 \\ 0 & e^{i\alpha(n)\gamma_n} \end{pmatrix}, \quad (22)$$

and $\gamma_n = z_n - z_{n-1}$, $n = 1, 2, \ldots, N$. It follows from (19) that the $A(0)$ and $B(0)$ amplitudes are related to $A(s)$ and $B(s)$ as

$$\begin{pmatrix} A(0) \\ B(0) \end{pmatrix} = \hat{M} \begin{pmatrix} A(s) \\ B(s) \end{pmatrix}, \quad (23)$$

where

$$M = \hat{T}_{01}\hat{T}_{12}\ldots\hat{T}_{N-1,N}\hat{T}_{Ns}, \quad (24)$$

$s \equiv N + 1$, and $\gamma_{N+1} \equiv 0$. On the assumption that electromagnetic waves are not reflected on the right side of the photonic crystal sample, the $t(\omega)$ transmission coefficient is given by the equation

$$t(\omega) = \left| \left(\frac{A(s)}{A(0)} \right)_{B(s)=0} \right|^2. \quad (25)$$

Using (23) yields

$$t(\omega) = \frac{1}{|\hat{M}_{11}|^2}, \quad (26)$$

where $\hat{M}_{11}$ is the $\hat{M}$ matrix element.

4. CALCULATION RESULTS AND DISCUSSION

Equations (9) and (10), which determine the frequencies and damping factors of localized modes of an infinite photonic crystal, were solved numerically. The results obtained for a photonic crystal with layer thicknesses $W_a = W_b = 1$ μm and layer permittivities $\varepsilon_a = 4$ and $\varepsilon_b = 2.25$, respectively, are given below. The refractive indexes of the defect layer in the IR region

$$n_d\left(\frac{\pi}{2}\right) = \sqrt{\varepsilon_\parallel} = n_\parallel = 1.7$$

and

$$n_d(0) = \sqrt{\varepsilon_\perp} = n_\perp = 1.5$$

corresponded to a 5TsB nematic liquid crystal at 20°C [25].

The electromagnetic excitation spectrum of an ideal layered medium has a band character [26]. A defect layer in a photonic crystal can cause the appearance of discrete frequencies within the forbidden bands of the unperturbed layered medium and electromagnetic field localization in defect modes. The dependences of the frequency and damping factor of defect modes in the second forbidden band ($n = 2$) on the thickness of the defect layer are shown in Fig. 2 for the normal and tangential orientations of the optical axis of the nematic. The frequencies

$$\omega_1 = 3.521\frac{c}{W} = 5.281 \times 10^{14} \text{ Hz}$$

and

$$\omega_2 = 3.663\frac{c}{W} = 5.495 \times 10^{14}\ \text{Hz}$$

in this figure determine the boundaries of the forbidden band spectral range. The change in the orientation of the director of the nematic not only substantially changes the frequency and damping factor of localized modes but can cause the appearance of new localized modes at certain defect layer thicknesses. Note that restoring translational invariance in the photonic crystal with $W_d = 1$ μm and $n_d = 1.5$ causes the disappearance of discrete frequencies within forbidden bands. An increase in the defect layer thickness at a given liquid crystal optical axis orientation increases the number of discrete frequencies in the photonic crystal forbidden band. At $W_d = 100$ μm, the number of localized modes at $\theta = 0$ and $\theta = \pi/2$ increases to five. At a qualitative level, this result can be given a visual explanation. Localized modes in the vicinity of defects in photonic band gap structures have much in common with cavity resonators. Indeed, a defect photonic crystal mode can be described as a standing wave formed as a result of reflection from semibounded superlattices, or, in other words, cavity walls. And the number of modes in a cavity in a given frequency range is proportional to its length.

Figure 3 illustrates the possibility of controlling the spectrum of defect modes and the spatial distribution of the square of the electric field modulus in photonic crystal defect modes with a $W_d = 4.5$ μm defect layer thickness. The center of the defect layer coincides with the origin. The curves at negative z values are obtained by mirror reflection in the $z = 0$ plane. The curve shown in Fig. 3b was constructed for $\theta = \pi/2$ and $n_{||} = 1.7$. The localized mode frequency near the forbidden band center then equals $\omega_L = 5.380 \times 10^{14}$ Hz, and the corresponding damping factor is $q = 0.125$. The localization of the square of the electric field modulus in the vicinity of the defect layer is clearly seen. Changing the orientation of the optical axis of the nematic from tangential to normal ($\theta = 0$, $n_\perp = 1.5$) causes the appearance of two defect modes near the continuous spectrum boundaries (Figs. 3a, 3c). The frequencies and the damping factors of the modes are $\omega_L = 5.491 \times 10^{14}$ Hz, $q = 0.026$ (Fig. 3a) and $\omega_L = 5.282 \times 10^{14}$ Hz, $q = 0.019$ (Fig. 3c). It follows that changes in the director orientation induce the appearance of new defect modes much less localized. Indeed, the mode damping factors (Figs. 3a, 3c) decrease 4.8 and 6.6 times, respectively. It follows from Fig. 2 that there exist defect layer thicknesses at which director reorientation from tangential to normal does not change the number of defect modes and only shifts their frequencies and damping factors.

Consider the special features of the transmission spectrum of a finite photonic crystal by numerically solving Eq. (26) for the transmission coefficient at various layered medium parameters. As with an infinite photonic crystal, we assume that $W_a = W_b = 1$ μm, $\varepsilon_a = 4$, and $\varepsilon_b = 2.25$.

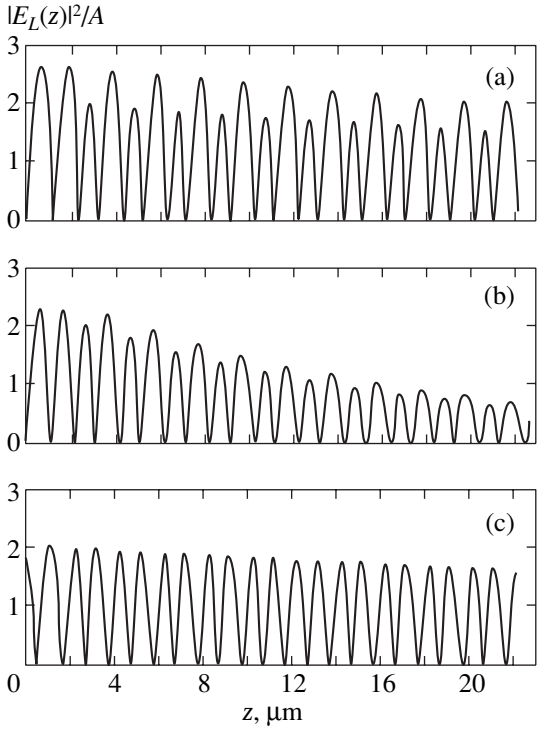

Fig. 3. The square of the electric field modulus of a localized mode. Defect layer thickness $W_d = 4.5$ μm, n_d = (a, c) 1.5 and (b) 1.7, $A = \left|A^r_{La}\right|^2$. The center of the defect layer coincides with the origin ($z = 0$).

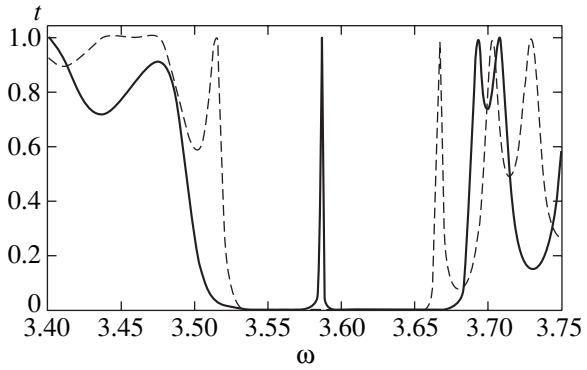

Fig. 4. Frequency dependence of the transmission coefficient of a photonic crystal with $N = 85$ layers. The thickness of the defect layer situated in the center of the layered medium is $W_d = 4.5$ μm. The dashed line corresponds to $n_d = 1.5$ at $\theta = 0$, and the solid line, to $n_d = 1.7$ at $\theta = \pi/2$; ω is in c/W units.

The frequency dependences of the photonic crystal transmission coefficient in the frequency range of the second forbidden band of the ideal photonic crystal at

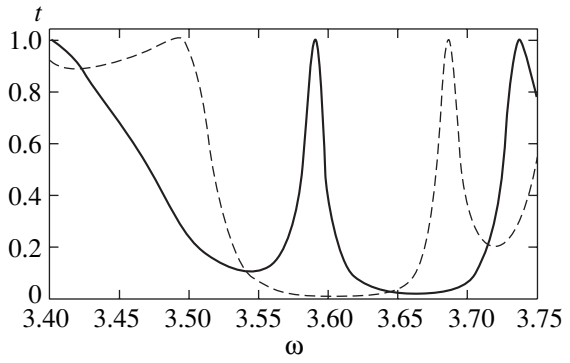

Fig. 5. Frequency dependences of the transmission coefficient of a sample with $N = 45$ layers. The defect is situated in the center of the photonic crystal. The other parameters have the same values as in Fig. 4; ω is in c/W units.

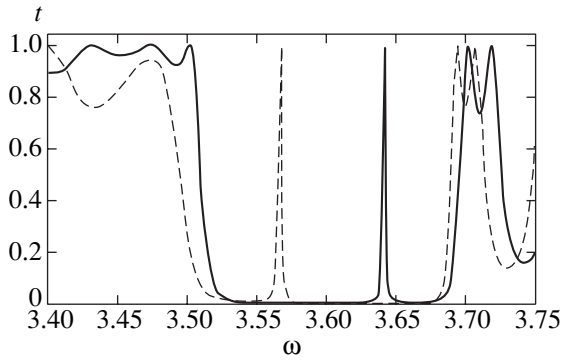

Fig. 6. Frequency dependences of the transmission coefficient of a photonic crystal with a defect layer of thickness $W_d = 5.2$ μm. The other parameters have the same values as in Fig. 4; ω is in c/W units.

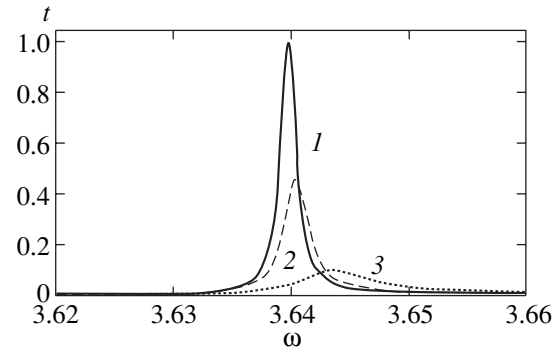

Fig. 7. Fragments of the transmission spectra of a photonic crystal at $\theta = \pi/2$ with various defect layer positions in the lattice. The defect is (*1*) in the center of the sample, $l = 43$, and at $l =$ (*2*) 33 and (*3*) 23. The other parameters are the same as in Fig. 6.

various nematic optical axis orientations are shown in Fig. 4. It follows from these dependences that the defect mode spectrum of a finite sample is close to the spectrum of localized modes in an infinite photonic crystal if the other layered structure parameters are equal (Figs. 2, 3). Indeed, at a $\theta = \pi/2$ orientation angle, a defect mode with an $\omega_L = 5.381 \times 10^{14}$ Hz frequency, which is close to the corresponding frequency of the defect layer in an infinite photonic crystal (Fig. 3b), appears in the transmission spectrum. The width of the transmission curve is about 10 Å. At $\theta = 0$, the transmission spectrum contains two defect modes with frequencies $\omega_L = 5.271 \times 10^{14}$ Hz and $\omega_L = 5.502 \times 10^{14}$ Hz. The frequency dependence of transmission for a sample with a smaller number of layers is shown in Fig. 5. A comparison of Figs. 5 and 4 shows that an almost twofold decrease in the number of layers in a photonic crystal with a lattice defect causes noticeable changes in the transmission spectrum. The transmission curves broaden, the position of the minimum changes, and the frequency corresponding to maximum transmission shifts.

It has been mentioned that, for an infinite photonic crystal, there exist defect layer thicknesses at which nematic optical axis reorientation shifts the frequency of the defect mode but does not cause the appearance of new defect levels in the forbidden band. An example is a photonic crystal with a $W_d = 5.2$ μm defect layer thickness (Fig. 2). For comparison, the frequency dependence of the transmission coefficient of a finite photonic crystal with a defect layer of the same thickness is shown in Fig. 6.

A characteristic feature of the curves shown in Figs. 4–6 is the high penetrating power of *H* waves. The transmission coefficient of *H* waves increases virtually to one when defect layers in the forbidden band appear. Note also that polarization of radiation that passes through photonic crystal samples with lattice defects can be controlled. Indeed, reorientation of the nematic liquid crystal optical axis from normal to tangential results in that *H*- and *E*-type modes acquire a phase difference after passage through the nematic layer.

Fragments of the transmission spectra of photonic crystals with different defect layer positions are shown in Fig. 7. The figure illustrates typical behavior of the transmission coefficient of *H* waves caused by the appearance of a defect level in the forbidden band when the defect layer is displaced from the symmetrical position to the boundary between the sample and the vacuum. We see that the transmission ability of the photonic crystal decreases, the transmission curve width increases, and the frequency of the defect mode slightly shifts. These effects can be given a simple physical interpretation. As mentioned, localized modes in the vicinity of the defect in a photonic crystal have much in common with a cavity resonator. The displacement of the defect to the boundary between the sample and the vacuum decreases the *Q* factor of the cavity, that is, modifies the transmission spectra of the photonic crystal.

Lastly, the transmission spectra of a photonic crystal with two differently spaced identical defect lattices are shown in Fig. 8. Increasing the distance between defect

layers causes qualitative changes in the transmission spectrum, namely, two transmission curves of defect modes coalesce; that is, localized electromagnetic modes become degenerate. Frequency degeneracy first appears for the normal orientation of the nematic liquid crystal director. Changes in the positions of transmission curve maxima can be qualitatively explained as follows.

The characteristic length determining the region of electromagnetic wave localization in the vicinity of a defect is $l = 1/q$. According to Fig. 2, $l(0) = 1/q \approx 17$ μm for $W_d = 5.2$ μm and $\theta = 0$ and $l(\pi/2) \approx 21$ μm for the same W_d thickness and $\theta = \pi/2$. When the distance between the defects approaches the characteristic length, $r \approx l$, two modes become strongly coupled, and their frequencies become split (Fig. 8a). Further, the distance between the defect mode frequencies increases as nematic liquid crystal layers approach each other. When the distance between the defects decreases to $r = 11.2$ μm, the high- and low-frequency defect mode transmission curves for $\theta = \pi/2$ and $\theta = 0$, respectively (Fig. 8a), coalesce with the continuous transmission spectrum of the photonic crystal. The modes are weakly coupled if the distance between the defects exceeds characteristic length l. The defect mode frequency is then doubly degenerate. At $\theta = 0$, the frequencies become degenerate at a smaller distance between the defects than when $\theta = \pi/2$ (Figs. 8b, 8c) because the corresponding characteristic localization lengths are related as $l(0) < l(\pi/2)$. Placing the defects $r = 71.2$ μm apart (the defects are then situated close to the boundaries between the photonic crystal and the vacuum) makes defect mode frequencies at $\theta = 0$ and $\theta = \pi/2$ doubly degenerate, the transmission curves of the localized modes are then strongly broadened, especially for $\theta = 0$, and maximum transmission coefficients are then much smaller than one. Note that if coupling between defect modes is close to critical (to coupling at which mode frequencies become degenerate), the transmission curve has a steep slope, and the transmission coefficient weakly depends on frequency (Fig. 8c, $\theta = \pi/2$). This circumstance can be used to create band filters.

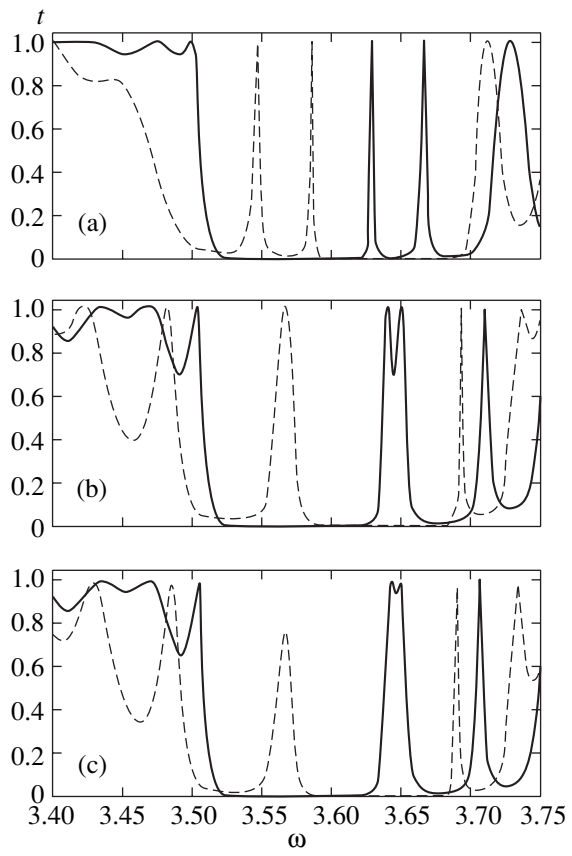

Fig. 8. Frequency dependences of the transmission coefficient of a photonic crystal with two defect layers. The number of layers in the sample $N = 87$, the other parameters are the same as in Fig. 4; (a) numbers of defect layers are $l_1 = 35$ and $l_2 = 53$, the distance between the layers is $r = 22.2$ μm, the defect modes are split; (b) $l_1 = 23$, $l_2 = 65$, and $r = 46.2$ μm, the frequencies for $\theta = 0$ are degenerate; and (c) $l_1 = 21$, $l_2 = 67$, and $r = 50.2$ μm, the frequencies are virtually degenerate also for $\theta = \pi/2$.

5. CONCLUSION

To summarize, we showed in this work that the spectrum of defect modes and the field distribution in defect modes of a one-dimensional photonic crystal had certain special features largely because of a strong permittivity anisotropy and a high sensitivity of the nematic, which played the role of a structural defect layer, to external fields.

Importantly, there exist liquid crystal layer thicknesses at which changes in the orientation of the nematic optical axis cause qualitative changes in the spectrum of defect modes, the appearance of new defect levels, and substantial changes in the degree of field localization in defect modes. We also showed that the transmission spectrum of a photonic crystal with one and two lattice defects experienced substantial rearrangement when the optical axis of the nematic liquid crystal was reoriented. In addition, the transmission spectrum of photonic crystals with two defects could be qualitatively modified by changing the distance between the defect layers in the lattice.

In practical applications, such photonic band gap structures offer promise for creating filters and polarizers with controllable characteristics. Lastly, note that the possibility of controlling the degree of localization of electromagnetic field along the direction of laser beam propagation appears to be promising for controlling the efficiency of nonlinear optical interactions.

REFERENCES

1. J. Joannopoulos, R. Meade, and J. Winn, *Photonic Crystals* (Princeton Univ. Press, Princeton, 1995).

2. E. Yablonovitch, Phys. Rev. Lett. **58**, 2059 (1987).
3. E. Yablonovitch, J. Opt. Soc. Am. B **10**, 283 (1993).
4. S. John and T. Quang, Phys. Rev. A **50**, 1764 (1994).
5. S. John, Phys. Rev. Lett. **53**, 2169 (1984).
6. S. John, Phys. Rev. Lett. **58**, 2486 (1987).
7. D. R. Smith, R. Dalichaouch, S. Schultz, *et al.*, J. Opt. Soc. Am. B **10**, 314 (1993).
8. S. Y. Lin, E. Chow, V. Hietala, *et al.*, Science **282**, 274 (1998).
9. A. M. Zheltikov, S. A. Magnitskiĭ, and A. V. Tarasishin, Pis'ma Zh. Éksp. Teor. Fiz. **70**, 323 (1999) [JETP Lett. **70**, 323 (1999)].
10. A. M. Zheltikov, S. A. Magnitskiĭ, and A. V. Tarasishin, Zh. Éksp. Teor. Fiz. **117**, 691 (2000) [JETP **90**, 600 (2000)].
11. M. Bayinder, B. Temelkuran, and E. Ozbay, Phys. Rev. B **61**, R11855 (2000).
12. B. Temelkuran and E. Ozbay, Appl. Phys. Lett. **74**, 486 (1999).
13. M. V. Alfimov, A. M. Zheltikov, A. A. Ivanov, *et al.*, Pis'ma Zh. Éksp. Teor. Fiz. **71**, 714 (2000) [JETP Lett. **71**, 489 (2000)].
14. M. Scalora, J. P. Dowling, C. M. Bowden, and M. J. Bloemer, Phys. Rev. Lett. **73**, 1368 (1994).
15. P. R. Villeneuve, D. S. Abrams, S. Van, and J. Joannopoulos, Opt. Lett. **21**, 2017 (1996).
16. A. Stingl, M. Jenzner, Ch. Spielmann, *et al.*, Opt. Lett. **20**, 602 (1995).
17. B. Temelkuran, E. Ozbay, J. P. Kavanaugh, *et al.*, Appl. Phys. Lett. **72**, 2376 (1998).
18. H. Kosaka, T. Kawashima, A. Tomita, *et al.*, Appl. Phys. Lett. **74**, 1370 (1999).
19. A. de Lustrac, F. Gadot, S. Cabaret, *et al.*, Appl. Phys. Lett. **75**, 1625 (1999).
20. K. Bush and S. John, Phys. Rev. Lett. **83**, 967 (1999).
21. S. Ya. Vetrov and A. V. Shabanov, Zh. Éksp. Teor. Fiz. **101**, 1340 (1992) [Sov. Phys. JETP **74**, 719 (1992)].
22. I. O. Bogul'skiĭ, S. Ya. Vetrov, and A. V. Shabanov, Opt. Spektrosk. **84**, 823 (1998) [Opt. Spectrosc. **84**, 742 (1998)].
23. K.-Q. Chen, X.-H. Wang, and B.-Y. Gu, Phys. Rev. B **61**, 12 075 (2000).
24. P. Yeh, J. Opt. Soc. Am. **69**, 742 (1979).
25. V. Ya. Zyryanov and V. Sh. Épshteĭn, Prib. Tekh. Éksp., No. 2, 164 (1987).
26. A. Yariv and P. Yeh, in *Optical Waves in Crystals: Propagation and Control of Laser Radiation* (Wiley, New York, 1984; Mir, Moscow, 1987), p. 169.

Translated by V. Sipachev